ELEVATED TEMPERATURE STRAIN GAGES

J.F. Lei, M. Shaarbaf, and J.O. Brittain
Northwestern University
Evanston, Illinois

The objective of this research is to study the electrical resistance of materials that are potentially useful as resistance strain gages at 1000°C. A set of criteria (1) were set and used to select strain gage candidate materials that are electrically stable and reproducible at all temperatures up to 1000°C. For the experimental phase of this research the electrical resistance change with temperature of three groups of materials (solid solution alloys, transition metal carbides and nitrides, and semiconductors) were studied with the intention of identifying materials with low temperature coefficient of resistance (TCR) and low resistance drift rate (DR) at 1000°C. A preliminary study of gage factor on one of the best candidates materials, B_4C, was also undertaken. The results of the investigation on these materials are presented in this report.

I. INTRODUCTION

A. Solid Solution Alloys

In previous report (1) a number of binary alloys were reported to have desirable electrical properties. These included alloys from Ag-Pd, Al-V, and Mo-Re systems. Since then the addition of third elements to these alloys has been made with the goal of decreasing TCR and DR at 1000°C. The third element(s) for each system was selected based upon Hume-Rothery's criteria for ideal solid solution (similar atomic radii, valance, and electronegativity) to avoid segregation or clustering which could have negative effects on electrical properties. The concentration ranges of these elements were selected by considering their solubility limits in the parent elements in each alloy in order to avoid formation of new phases.

B. Transition Metal Compounds

The refractory carbides and nitrides of the transition metals comprise a class of compounds with many scientifically interesting and useful properties such as: high melting temperatures ($\simeq$ 3000°C), high electrical conductivity, great hardness, wide homogeneity range, and excellent chemical stability. The transition metals in these compounds are from groups IV (Ti, Zr, Hf), V (V, Nb, Ta), and VI (Cr, Mo, W) of the periodic table. However, not all the carbides and nitrides of these elements seemed to be suitable for high temperature resistance strain gage application. Among these materials, nitrides of group VI were excluded from list of potential compounds because they dissociate rapidly at high temperatures. VN, NbN, MoC and WC were also excluded due to their complex phase diagrams and narrow ranges of homogeneity.

A wide homogeneity range is characteristic of the cubic transition metal compounds. For all rocksalt structured transition metal carbides, nonstoichiometry is due to carbon vacancies only and the metallic sublattice remains completely occupied, as shown by precise density measurements (2). Some mononitrides such as TiN_x are reported to be nonstoichiometry with x values larger than 1. These compounds are characterized as containing metal vacancies whose concentration increases with an increase in x, that is for a nitrogen concentration > 1 (4). The presence of a large concentration of vacancies would be expected to affect various physical properties. In this research the effect of vacancy concentration on the electrical properties of these transition metal compounds was also investigated in order to select the proper strain gage candidates among them.

C. Semiconducting Materials

Traditional semiconductor resistance strain gages are made of silicon or germanium, which have band gaps of 1.11 and 0.67 eV, respectively. In order to extend the working temperature of the strain gages to higher temperatures, semiconducting materials with band gaps larger than 1.11 eV are therefore needed. α-SiC, β-SiC and B_4C with band gaps of 2.86, 2.3 and 2.5 eV, respectively, were chosen for this study. Their intrinsic conduction occurs at temperatures above 1000°C.

II. MATERIALS PREPARATION, PROCESSING AND EXPERIMENTAL TECHNIQUE

The alloys listed in Table I were prepared by arc melting and remelting (about 5 times) charges of about 5 grams under purified argon atmosphere. The ingots were then cut by electrical discharge mechining into rectangular samples of 8x3x1 mm for electrical resistance measurements.

The specimens of transition metal compounds and β-SiC were prepared as thin films on Al_2O_3 substrates by several different evaporation or sputtering techniques, listed in Table II. All films were cut into samples about 15 mm long by 1.5 mm wide via a diamond blade. Boron carbide and α-silicon carbide bulk samples prepared by hot pressing were thinned by slicing into 15x1.5x1 mm specimens via a diamond cut-off wheel.

Specimens for electrical resistance measurements were chemically cleaned to remove any debris and contaminations. These samples were then encapsulated in quartz tubings under vacuum and were subsequently annealed for one day at slightly above 1000°C followed by furnace cooling to room temperature. The electrical resistance (ER) of two or three specimens were measured simultaneously via a four probe technique as described in previous report (1) in the temperature range of 23-1000°C under vacuum ($2x10^{-5}$ torr). The ER of boron carbide in air was also measured.

A device which consisted of a constant strain cantilever beam designed first by McClintock (3) was adopted and modified (Fig. 1) to measure the gage factor of materials. Samples were attached to the surface of the cantilever

beam by means of a high temperature ceramic adhesive (AREMCO products). The stepped, sliding block which is in contact with the free end of the beam via a screw was accurately machined so that the difference in height between any two steps represents a known deflection of the free end of the beam, and consequently a known strain at the beam surface (Fig. 2). The sliding block, beam, frame and screws were all made of the same material (Aremcolox high temperature low thermal expansion machinable ceramics) to minimize relative dimensional changes of these parts resulting from the thermal expansion.

III. RESULTS — Solid Solution Alloys

Additions of third elements to the alloys of the following systems resulted in similar ER-T curves as their parent binary alloys. A metallographic examination indicated that these elements did not result in the formation of any new phases in these alloys.

A. Palladium-Silver System

Experimental results on Pd-Ag alloys (1) showed an increase in Ag content from 4.1 to 15.5 st.% reduced the TCR from 774 to 250 ppm/^{o}C without a significant change in reproducibility. This is in agreement with the published data for Pd-Ag alloys (4). Based on these observations the Pd-12 wt.% Ag alloys was selected to be doped by small additions of Ni to verify the effects of Ni on the electrical properties of these alloys. Fig. 3 shows the ER-T data for Pd-12 wt.% Ag-7 Ni alloy. Addition of Ni as a third element had a positive effect on TCR and DR of these alloys, Table 1. Figure 4 shows that an increase in Ni content resulted in systematic decrease in TCR.

B. Aluminum-Vanadium System

The experimental results of the investigated binary Al-V alloys (1) indicated that these alloys generally have low TCR values but undesirable drifts in ER at high temperatures. However, Al-79.3 wt.% V containing a small amount of Si had a very low TCR (-22 ppm/C) and drift (50 ppm/hr) at 1000^{o}C. This prompted an investigation of the effect of additions of third elements to these alloys. In this work the effects of Mo and Cr as third elements on electrical properties of Al-79.3 wt.% were investigated. Figures 5 and 6 show ER-T data for Al-79.3 wt.% V-4.25 wt.% Mo alloy and the effect of Mo content on TCR of these alloys. An increase in Mo content had a beneficial effect in these alloys as it resulted in lower TCR and drift values (Table I). On the other hand Cr is not a suitable ternary element for this system. Increasing the Cr content in Al-79.3 wt.% V-Cr alloys resulted in larger negative TCR values with no significant change in drift (Table I) in electrical resistance at high temperatures. Figures 7 and 8 show the ER-T data for Al-79.3 wt.% V-1.75 wt.% Cr alloy along with TCR vs Cr content of these alloys, respectively.

C. Niobium-Vanadium System

In previous report Nb-5.2 wt.% alloy was investigated based on its reported good oxidation resistance (5) but its rather large TCR (550 ppm/k) and drift (550 ppm/hr) values were less than desirable. Despite these observations this system was selected as a good candidate for further studies and Mo was selected as the ternary element for this system. Figure 9 shows the ER-T data for Nb-8 wt.% V-7 Mo alloy. Nb-V-Mo alloys studied all showed good reproducibility (low drift). However, Mo additions resulted in increase in TCR values for these alloys (Fig. 10).

IV. SUMMARY — Solid Solution Alloys

It was intended to study the general effects of selected ternary elements on the electrical properties of a number of alloy systems which in terms of low TCR (< 300 ppm/C) values seemed promising. The objective was to identify the most desirable third element for a specific alloy and the best concentration of the third element in that alloy.

In the case of Pd-Ag alloys, Ni has been found to be a suitable third element and addition of this element to Pd-Ag alloys with higher Ag contents (> 12 wt.%) may result in practically low TCR values.

All of the Al-V-Mo alloys meet the TCR requirements of < 300 ppm/C. The alloys with higher Mo content had lower drift values, in particular, Al-79.3 wt.% V-4.25 wt.% Mo had the best TCR (-19 ppm/C) and drift (103 ppm/hr) combination. Further study on this system with higher Mo content is planned. Because of the negative effects of Cr on Al-V alloys no further work is planned for this system incorporating Cr.

Addition of Mo resulted in negative effect on the electrical properties of Nb-V alloys. However, further work is underway on effect of other third elements on these alloys as well as the Mo-Re alloys.

V. RESULTS — Refractory Compounds

A. Transition Metal Compounds

The results of change in its ER with change in temperatures for two TiN_x, two TaN_x, three ZrN_x, two TiC_x and ZrN_x films with different x's were presented in last report (1). The ER-T curves for ZrC is shown in figure 11, and the comparison between results of three TaN_x and four ZrN_x films are shown in the figures 12 and 13, respectively. The compositions of these transition metal compound films were characterized by means of x-ray, SEM, and Auger electron spectroscopy. The experimental results of these transition metal compounds are summarized in Table III, including TCR (at 1000°C), DR (at 1000°C), resistivity (at room temperature), composition and the partial pressure of nitrogen (carbon) during preparation. From these results it is suggested that:

(1) TCR and DR of the stoichiometric carbides were lower than those of their corresponding stoichiometric nitrides, e.g., TCR of TiC was lower than that of TiN and TCR of ZrC was lower than that of ZrN, as shown in figure 14.

(2) TCR of stoichiometric ZrN was lower than that of TiN and TCR of ZrC is lower than that of TiC, also shown in figure 14. These results indicate that the TCR of transition metal nitrides and carbides with transition metals in the same column of the period table decreased as quantum number of the transition metal increased.

(3) The resistivities of these compounds increased while their TCC decreased with increasing the vacancy concentration, as shown in Table III and figure 12.

(4) As shown in figure 15 the TCR of these transition metal compounds decreased as the resistivities of the compounds increased. Extrapolation of the data in figure 15 suggests that TCR passed through zero at resistivity of about 800-1000 microohm-cm.

(5) High temperature resistance saturations were observed in the Zr-C and ZrN systems. These two samples had larger resistivities (in the range of 180 and 560 microohm-cm) that resulted from stronger vacancy scatterings among all of the specimens studied except $TiN_{0.9}$ which had a resistivity of 1130 microohm-cm and a negative TCR. The ER-T behaviors of ZrN and ZrC fitted a "parallel resistor" formula (6)

$$1/R(T) = 1/R(\text{ideal}) + 1/R_{max}$$

where $R(\text{ideal}) = R_o + bT$, R_o is the residual resistance, b is fitting parameter and R_{max} is the apparent saturation value of the resistance at high temperatures. Plots of $(R_{max} \times R)/(R_{max} - R)$ versus temperature for ZrN and ZrC were made and shown in figures 16 and 17, respectively, where R_{max} corresponded to a resistivity of 1000 microohm-cm. The value of this saturation resistivity (1000 microohm-cm) was about the same as that when TCR vs resistivity curve (Fig. 15) passes through zero TCR.

(6) The presence of both a small TCR and a small DR value seemed to be mutually exclusive. However, the source of the high temperature resistance drift for the materials investigated was not ascertained. Note that pure platinum also displayed a high DR ($\simeq$ 0.2 %/hr).

B. Semiconductors

Table IV summarized the experimental results for the B_4C, β-SiC and α-SiC. The ER-T curves of B_4C, β-SiC-1 and α-SiC tested in a vacuum were presented in previous report (1). Since B_4C looked promising, it was therefore also tested in the air, its ER-T curve shown in Fig. 18. β-SiC-2 which had some N_2 dopants was also tested (in the vacuum) to study the doping effect, this is shown in Fig. 19. The results of these semiconductors can be summarized as follows:

(1) The change in resistance of B_4C with temperature followed a form of $R=AT \exp (E_A/kT)$, with activation energy (E_A) of about 0.14±0.005 eV, shown in Fig. 20. The temperature dependence of resistance in B_4C is actually the temperature dependence of its mobility (7), and the activation energy was large so that its mobility had a weakly temperature dependent value and resulted in a small TCR value at high temperatures.

(2) β-SiC had a weaker temperature dependence of resistance compared with α-SiC, and it is a more promising strain gage material for use at high temperatures. The TCR of β-SiC was decreased by doping, however, the DR showed a slight increase.

C. Gage Factor Measurement

The gage factor measurement system was first calibrated with three commercial resistance strain gage (Micro-Measurements Co.) at room temperature. Then a hot pressed B_4C was attached to the cantilever beam with a ceramic adhesive and tested in the vacuumed furnace. The change in its resistance with temperature was compared to that of the resistance data from a sample without applying adhesive as shown in Fig. 21, the consistence between the two curves indicates the inertness of the adhesive.

Figure 22 illustrates the resistance versus strain characteristics for boron carbide at three different temperatures. A linear change in resistance with applied strain at strain levels of 306 microstrain was observed. The gage factor drift at 1000°C was found to be about 0.22 %/hr for a period of 6 hours.

Figure 23 is a plot of percentage change in gage factor from its room temperature value versus temperature for B_4C in the temperature range of 23°C to 1000°C. This figure shows that the gage factor of B_4C decreased with increasing temperature. The gage factor was about 196±1% at 1000°C and 455±2% at room temperature. It varied by about 57% from room temperature to 1000°C. The gage factor of Wu's Chinese gage (8) was 2.56 at room temperature and 1.9 at 700°C, a variation of about 26% in the temperature range from room temperature to 700°C. In the same temperature range the gage factor variation for B_4C was about 32%. Since no effort has been made to optimize the performance of B_4C, the comparison is rather favorable. The reproducibility of gage factor of B_4C and its gage factor behavior under higher strain are planned for further studies.

VI. SUMMARY — Refractory Compounds

The low values of TCR of transition metal compounds were associated with highly defective lattice structures. However, structures with high concentration of defects were often unstable at high temperatures. Therefore, the selection of the composition of these transition metal compounds depends on which one of the two factors is more dominate, lower TCR or better stability.

Based upon the data presented in Table III and IV which summarize the

experimental results, we conclude that TiC, ZrC, B_4C and β-SiC have the potential to be used in production of high temperature resistance strain gages due to their low TCR and good stability. However, further studies on the optimization of their electrical behaviors and protection of these materials from oxidation at high temperature is necessary before these materials could be utilized in strain gage.

REFERENCES

1. Brittain, J. O.; Geslin, D.; and Lei, J. F.: Elevated Temperature Strain Gages, Proceedings of a Conference on Turbine Engine Hot Section Technology 1986, NASA Conference Publication 2444.

2. Storms, E. K.: The Refractory Carbides, Academic Press, N.Y. and London, 1967.

3. McClintock, R. M.: Strain Gage Calibration Device for Extreme Temperature. The Review of Scientific Instruments, Vol. 30, no. 8, 1959, pp. 715-718.

4. Schroder, K.: Handbook of Electrical Resistivities of Binary Metallic Alloys, CRC Press, 1983.

5. Lazarev, E.; and Eklind, G. S.: (Moscos) Izv. Akad. Nauk. SSSR, Met. (4), 1979.

6. Dy, L. C.; and Williams, W. S.: Resistivity, Superconductivity, and Order-Disorder Transformations in Transition Metal Carbides and Hydrogen-Doped Carbides, J. Appl. Phys., vol. 53, no. 12, 1982, pp. 8915-8927.

7. Wood, C.; and Emin, D.: Conduction Mechanism in Boron Carbides, Phys. Rev., vol. B29, no. 8, 1984, pp. 4582-4597.

8. Hobart, H. F.: Evaluation Results of the 700°C Chinese Strain Gages, NASA Conference publication 2443, 1985, pp. 77-84.

TABLE I. SUMMARIZED RESULTS FOR ALLOYS

Alloy	wt.%	TCR (1000°C)(ppm/C) Cycle 2 Heating	Cooling	Drift (1000°C)(ppm/hr)
Pd-12Ag-Ni	1 Ni	407	424	5080
	3	392	415	3640
	5	390	380	1163
	7	375	394	1460
Al-79.3V-Mo	.25 Mo	-113	-129	687
	.75	- 57	- 49	837
	2.25	- 27	- 31	54
	4.25	- 20	- 13	103
Al-79.3V-Cr	.25 Cr	- 28	- 8	- 74
	.75	- 44	- 80	-176
	1.25	- 75	-106	130
	1.75	-107	- 95	170
	2.25	- 22	- 34	-140
	2.75	-114	-125	- 70
Nb-8V-Mo	1 Mo	436	450	360
	3	540	550	400
	5	523	487	484
	7	557	528	115

TABLE II. PREPARATION METHODS FOR CANDIDATE MATERIALS*

Specimen	Preparation Method	Remarks
TiN-1	HCD, Hollow Cathode Discharge	
-2	CVD, Chemical Vapor Deposition	
ZrN-1		P_{N_2} = 114 ppm-torr
-2	RFS, Radio Frequency Sputtering	= 108 ppm-torr
-3		= 96 ppm-torr
-4		= 990 ppm-torr
TaN-1		P_{N_2} = 330 ppm-torr
-2	Magnetron RFS	= 375 ppm-torr
-3		= 600 ppm-torr
CrN	HCD	
TiC-1	ARE, Activated Reactive Evaporation	
-2	CVD	
ZrC	ARE	
B_4C	Hot Pressed	Bulk
β-SiC-1	EBE, Electron Beam Evaporation	
-2	CVD	with N_2 dopant
α-SiC	Hot Pressed	Bulk

*all the specimens are prepared as thin films on the Al_2O_3 substrates except for B_4C, α-SiC and CVD prepared β-SiC on Si substrate.

TABLE III. SUMMARIZED RESULTS FOR TRANSITION METAL COMPOUND MX_x

Specimen	P_{N_2} (μtorr)	X/M	Resistivity (μohm-cm)	TCR* (ppm/°C)	DR* (%/hr)
TiN(HCD)		1	30.5	588	0.14
(CVD)		0.9 (V_N)	1130	143	0.22
ZrN-1	114	≈1 (V_N)	180	275	-0.26
-2	108	<1 ↓	211	228	-0.36
-3	96	<<1 +	255	184	1.6
-4	990	≈1.10 (V_{Zr})	393	212	-0.54
TaN-1	330	+	113	255	0.53
-2	375	↑	103	301	0.5
-3	600	(V_N)	165	438	-0.16
CrN			13.8	710	2%
TiC(ARE)		≈1	39.4	338	0.06
(CVD)		0.8 (V_C)	169	210	-0.5
ZrC		0.76 (V_C) or 0.9	560	180	-0.13

*TCR and DR values are based on the data of 1000°C and DR were measured after cycle two heating.

TABLE IV. SUMMARIZED RESULTS FOR SEMICONDUCTING CANDIDATE MATERIALS

Specimen	ρ (Ω-cm)	TCR (ppm/^{o}C)	DR (%/hr)	Remarks
B_4C	0.24	-200	0.095	tested in vacuum
		-250	0.9	tested in air
				hot pressed bulk
β-SiC-1	0.01	-330	-0.32	"pure" 0.25 μm thick, prepared by EBE
-2	0.2	-223	-0.53	with N_2 dopants 7 μm thick prepared by CVD
α-SiC	10.1	-2100	0.04	hot pressed bulk

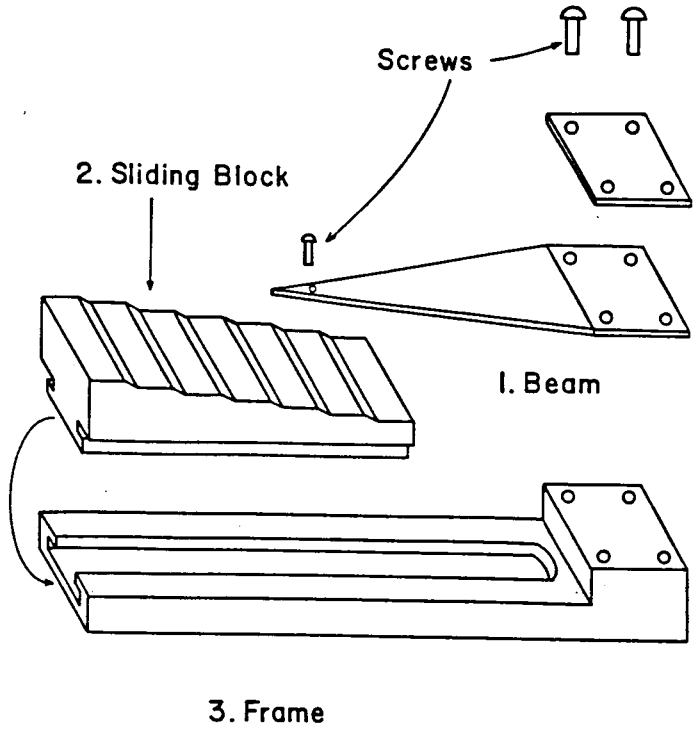

Fig. 1. Schematic diagram of the apparatus for gage factor measurements.

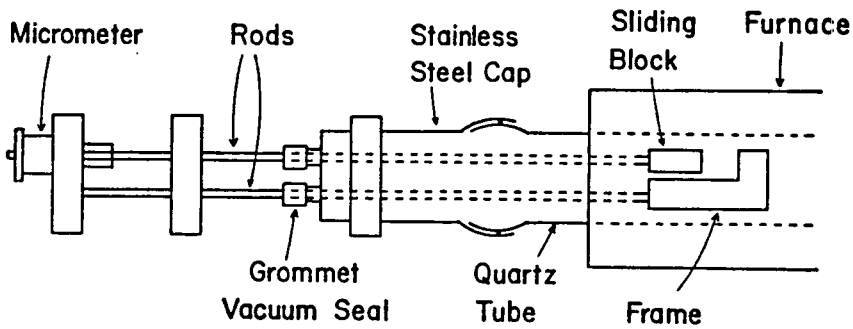

Fig. 2. Schematic diagram of the arrangement for actuating the sliding block to apply a strain to the specimen.

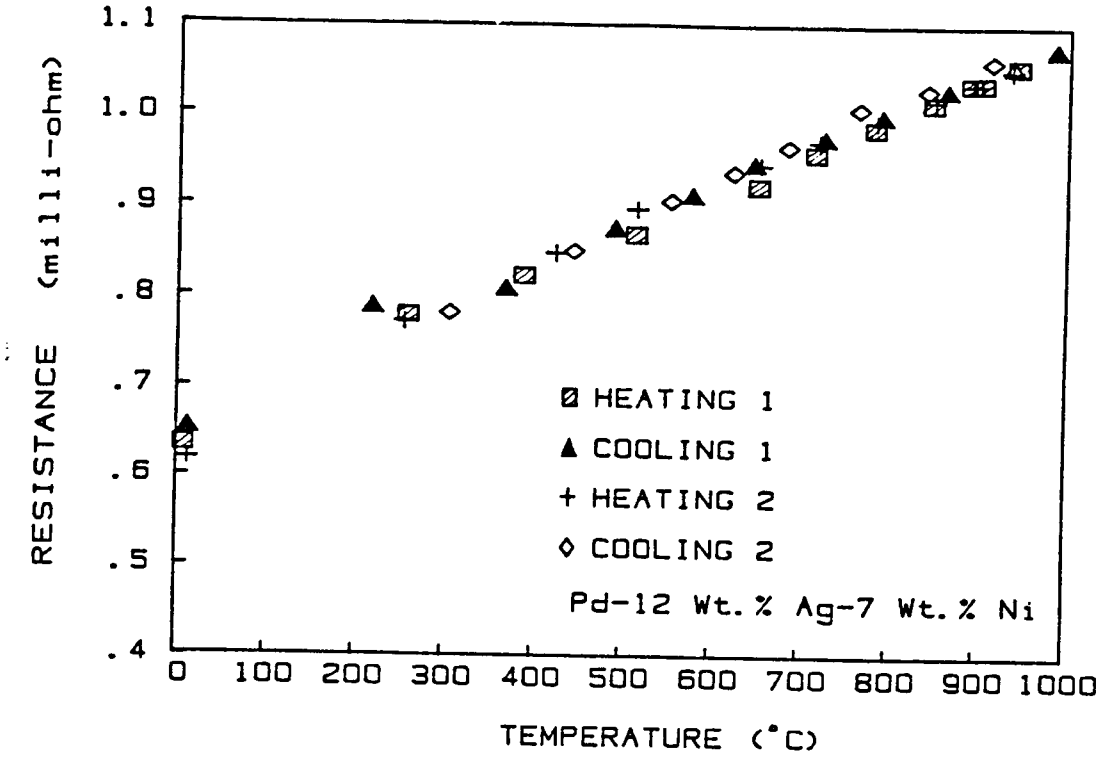

Fig. 3 RESISTANCE vs. TEMPERATURE

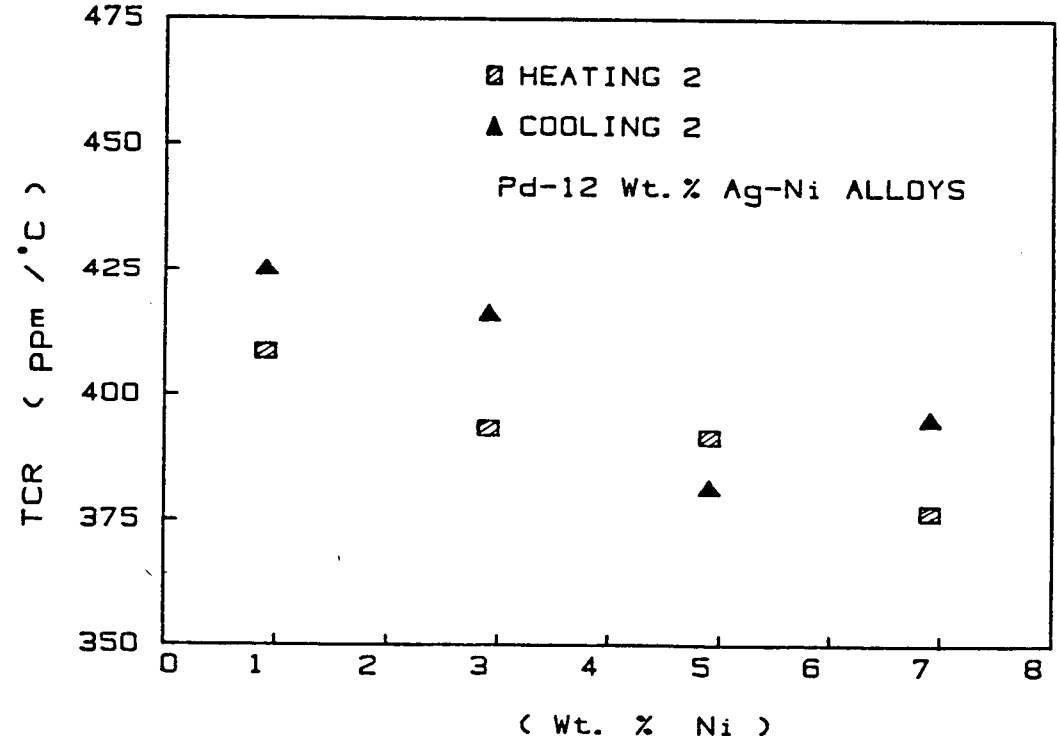

Fig. 4 TCR (1000°C) vs. Wt.% Ni

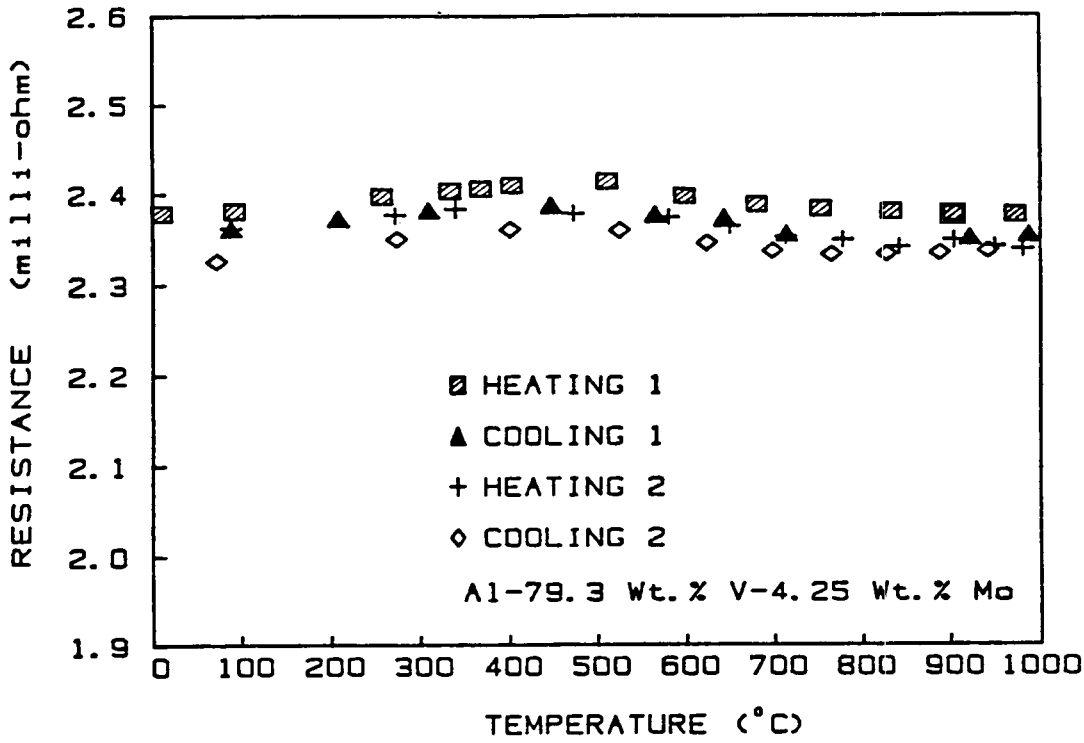

Fig. 5 RESISTANCE vs. TEMPERATURE

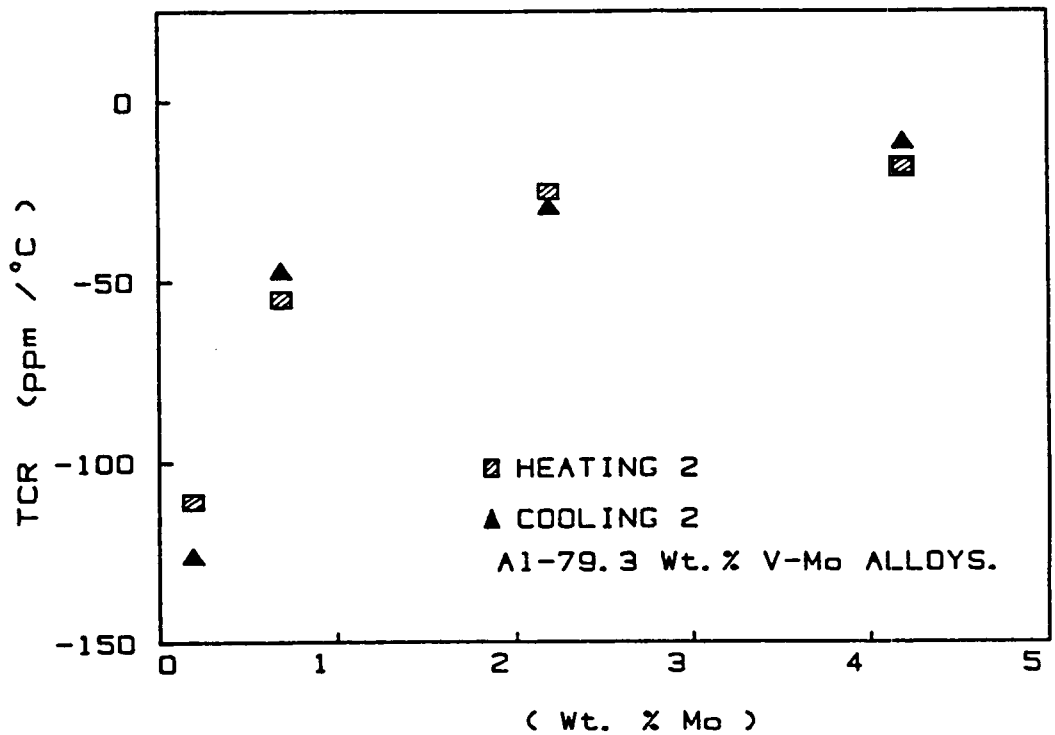

Fig. 6 TCR (1000°C) vs. Wt.% Mo

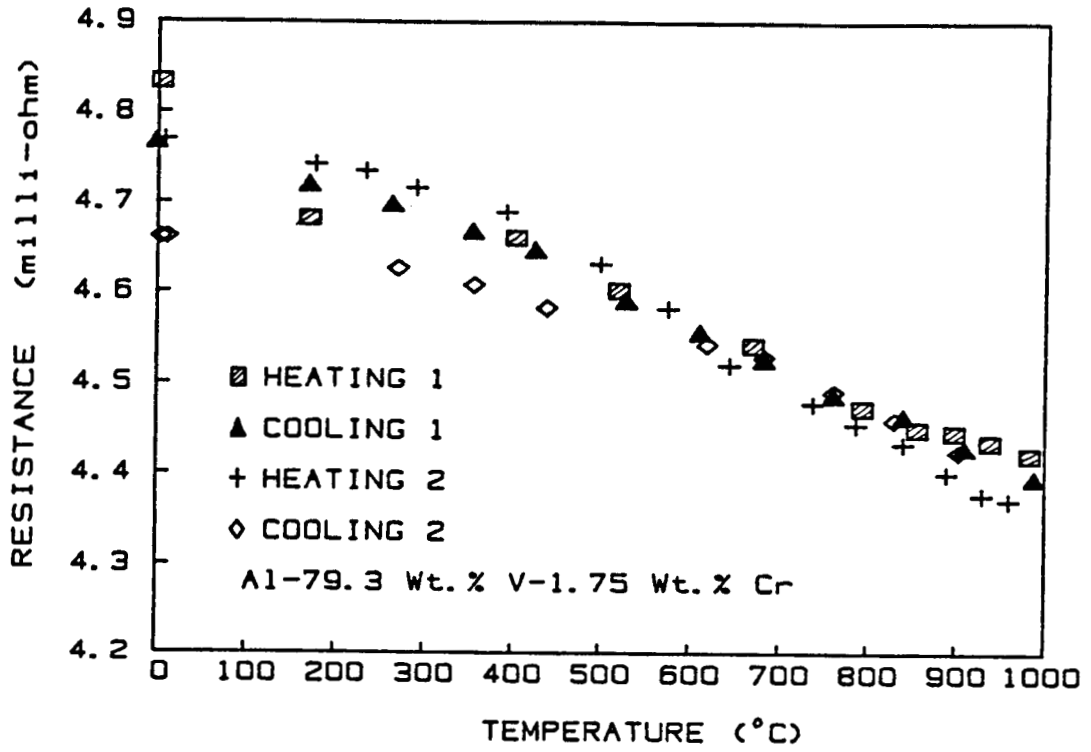

Fig. 7 RESISTANCE vs. TEMPERATURE

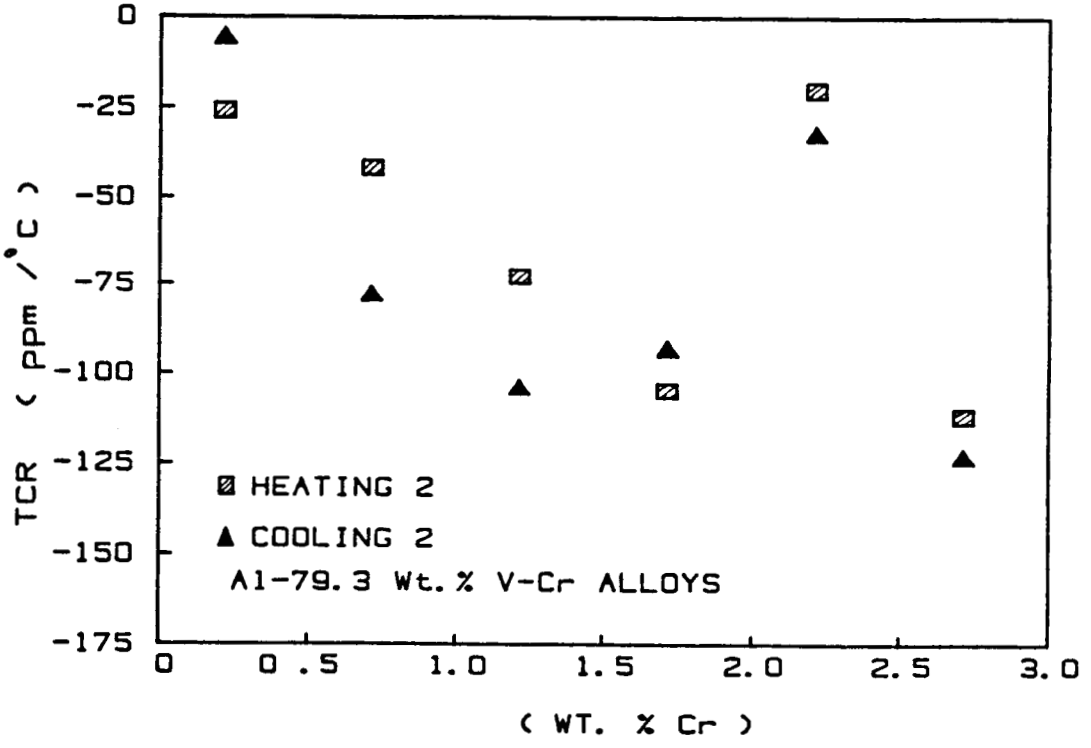

Fig. 8 TCR (1000 °C) vs. Wt.% Cr

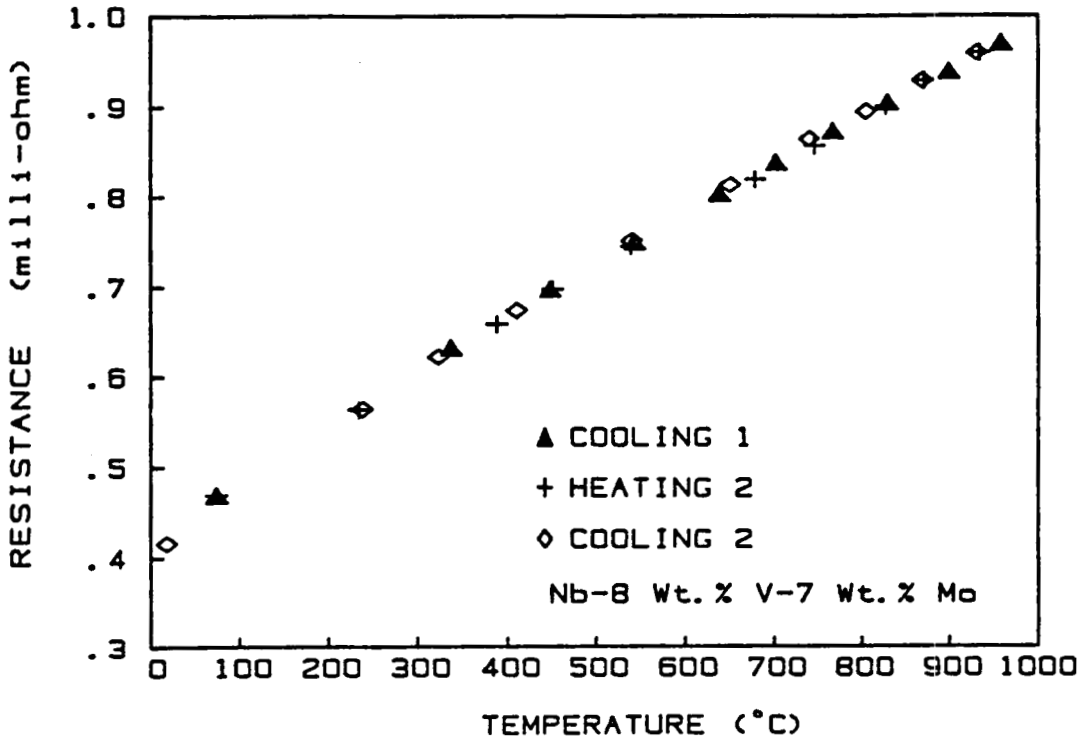

Fig. 9 RESISTANCE vs. TEMPERATURE

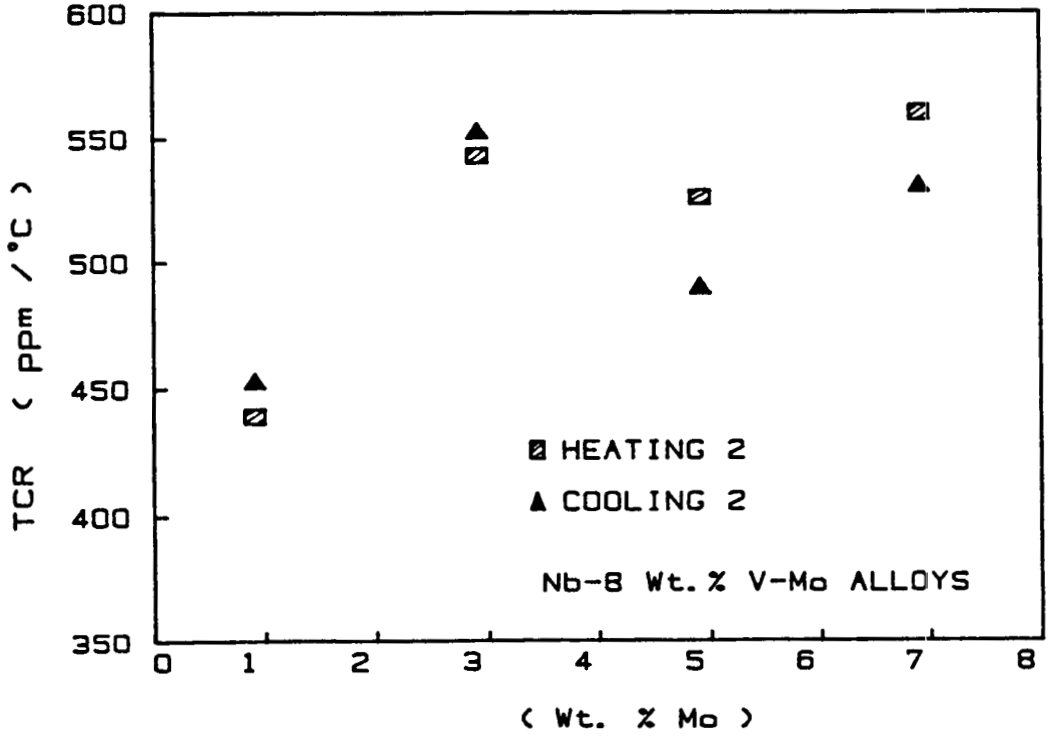

Fig. 10 TCR (1000°C) vs. Wt.% Mo

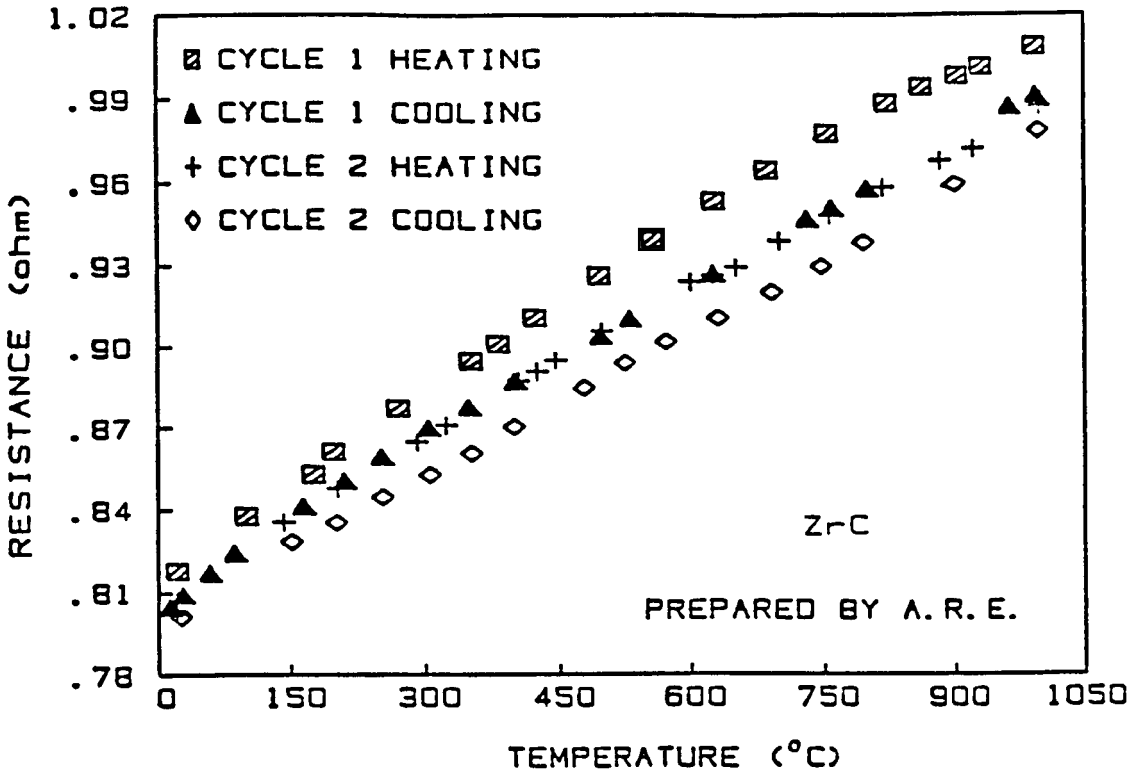

Fig. 11. Resistance vs. temperature of zirconium carbide.

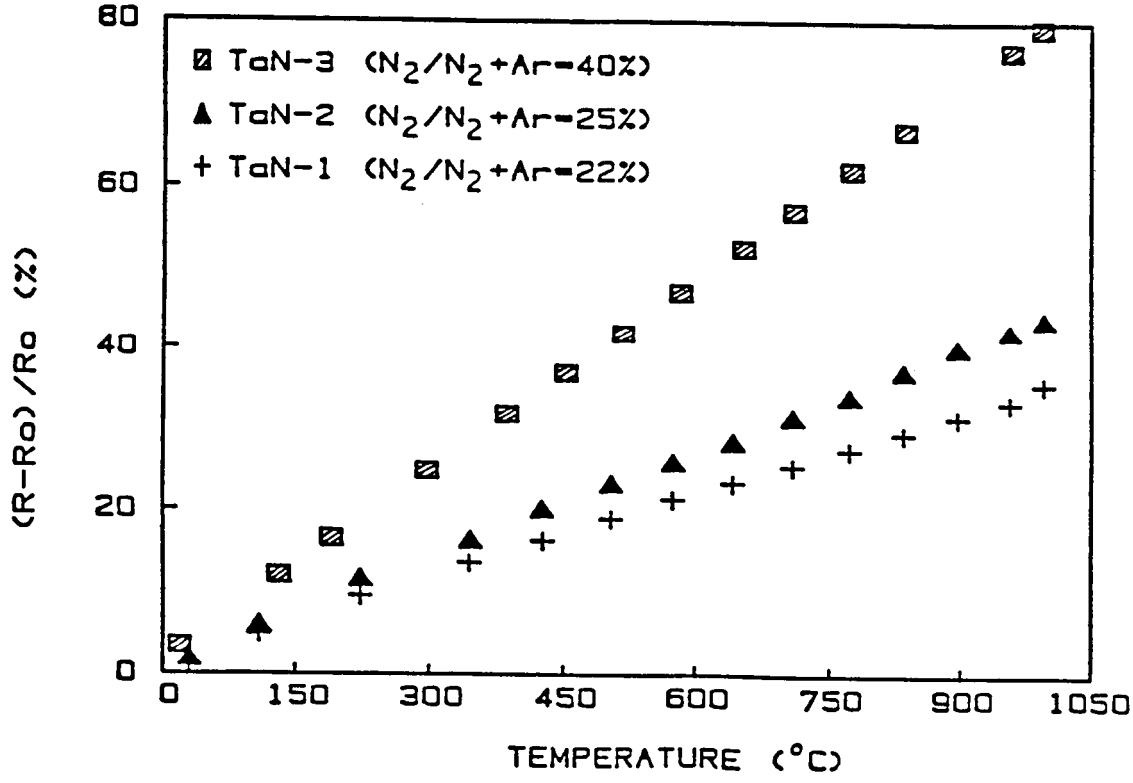

Fig. 12. Comparison the change in resistance with temperature for three tantalum nitrides.

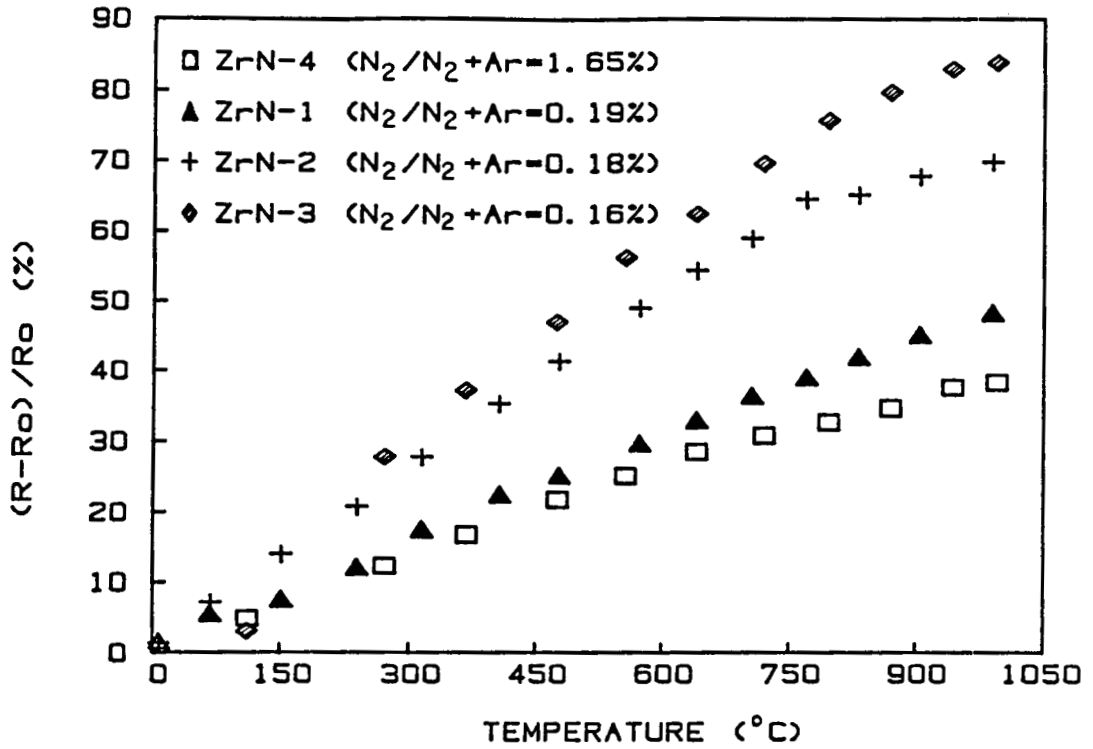

Fig. 13. Comparison the change in resistance with temperature for four zirconium nitrides.

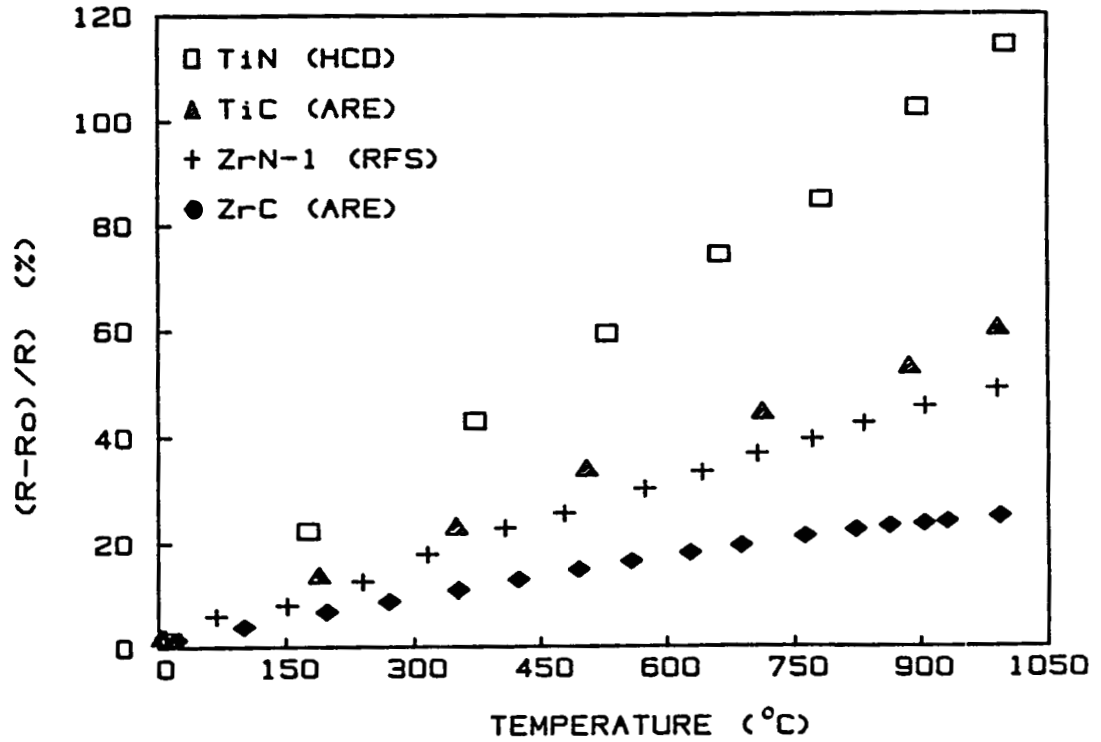

Fig. 14. Comparison the resistance change with temperature for TiC and TiN; ZrC and ZrN.

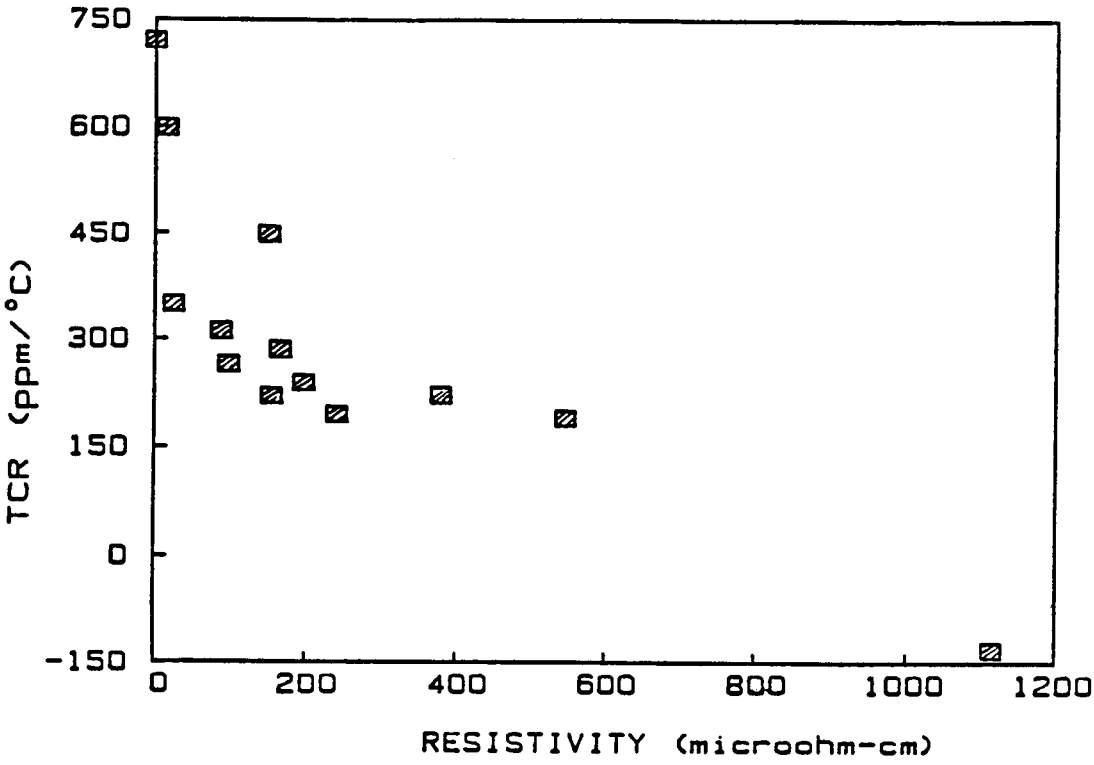

Fig. 15. TCR vs. resistivity for transition metal compounds.

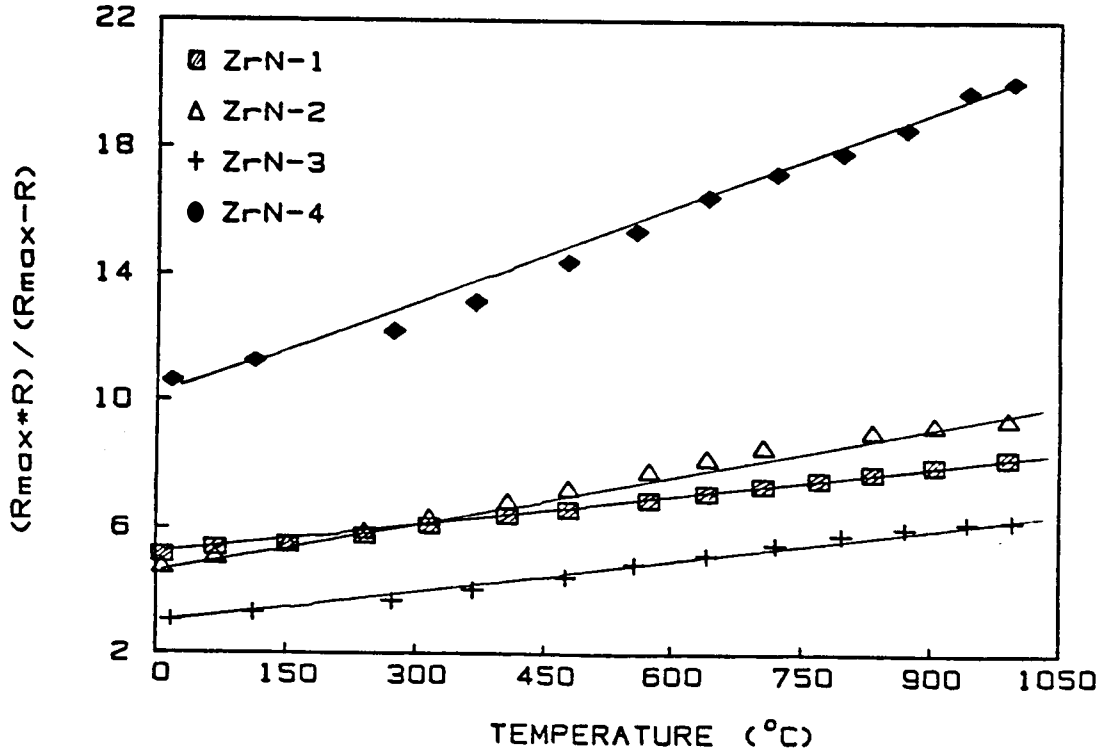

Fig. 16. (Rmax x R) / (Rmax-R) vs. temperature for four ZrN. Rmax correspondes to ρ_{max} = 1000 microohm-cm.

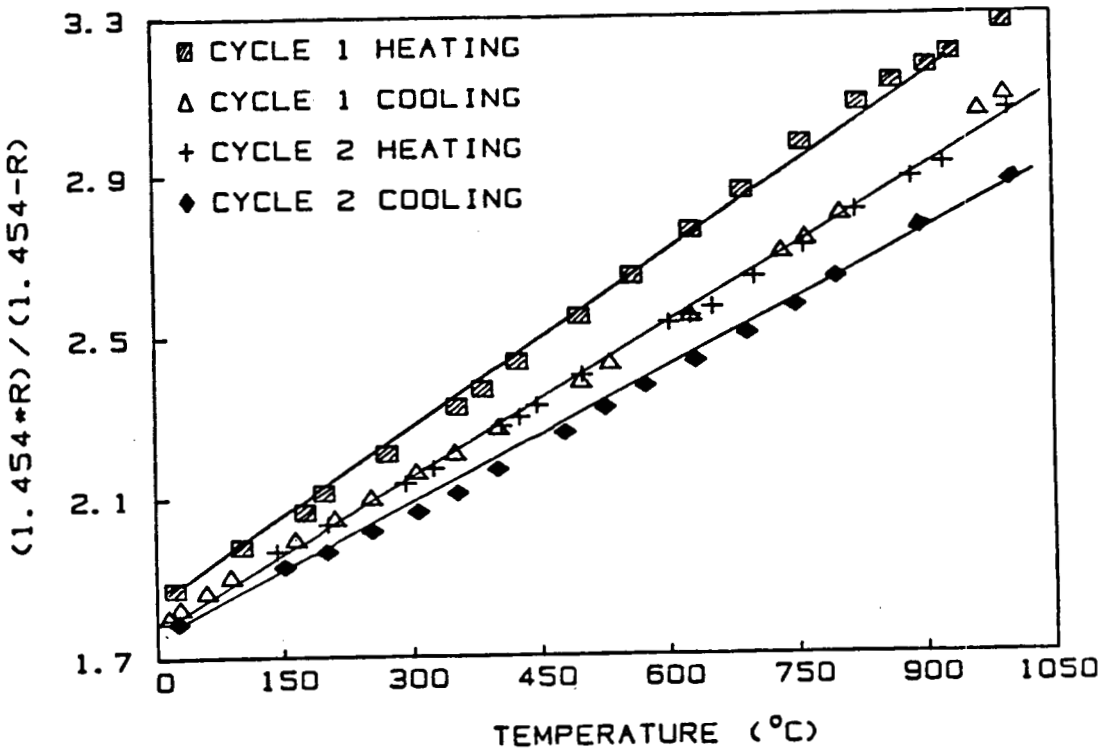

Fig. 17. (Rmax x R)/(Rmax-R) vs. temperature for ZrC.
Rmax=1.454 ohm correspondes to max = 1000 microohm-cm.

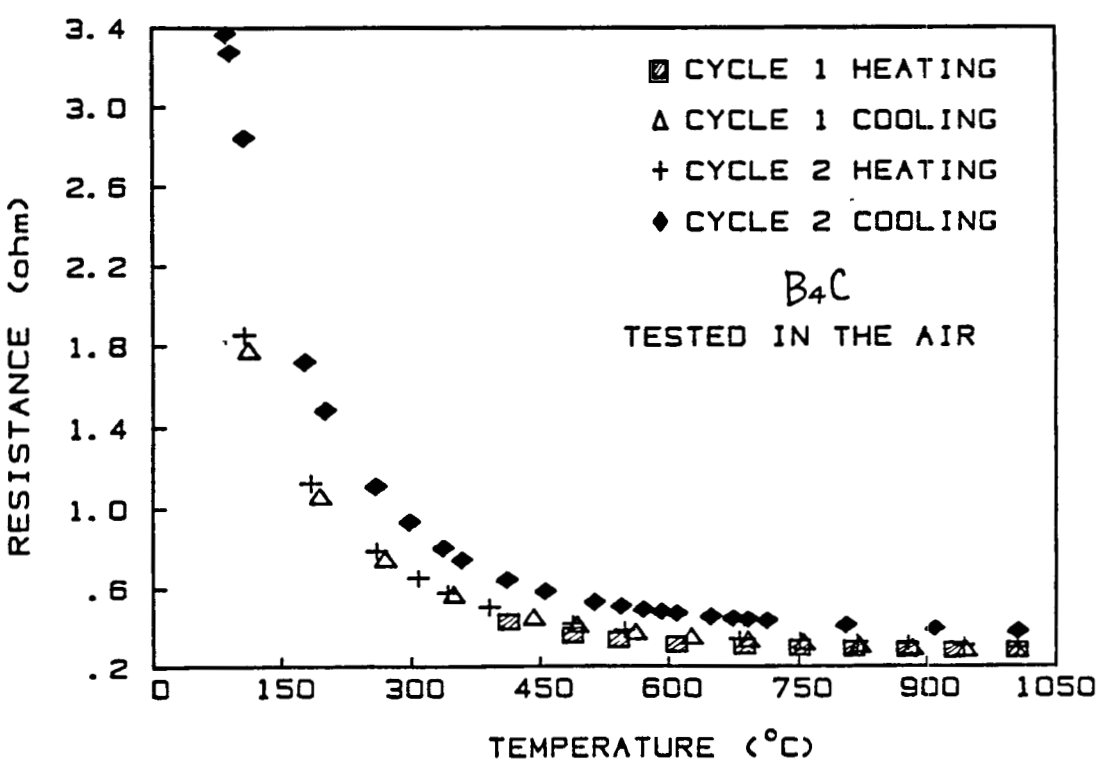

Fig. 18. Resistance vs. temperature for boron carbide tested in the air

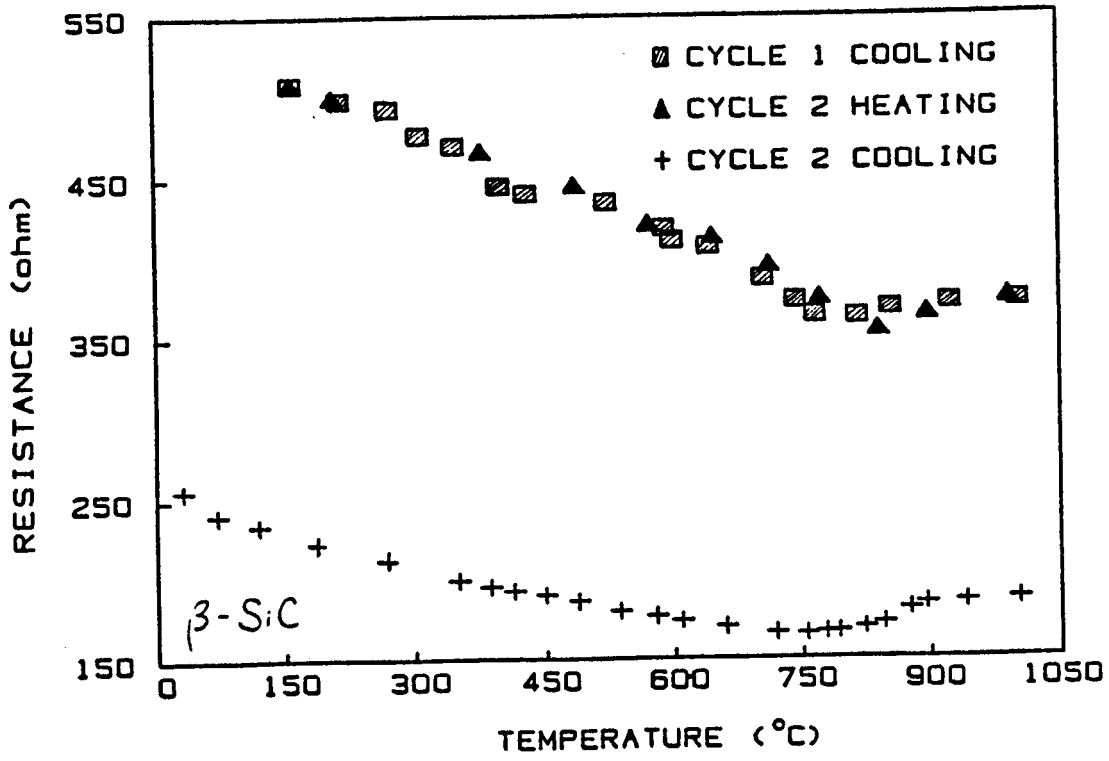

Fig. 19. Resistance vs. temperature for β-SiC film on the Al_2O_3 substrate. Film was porpared by CVD method.

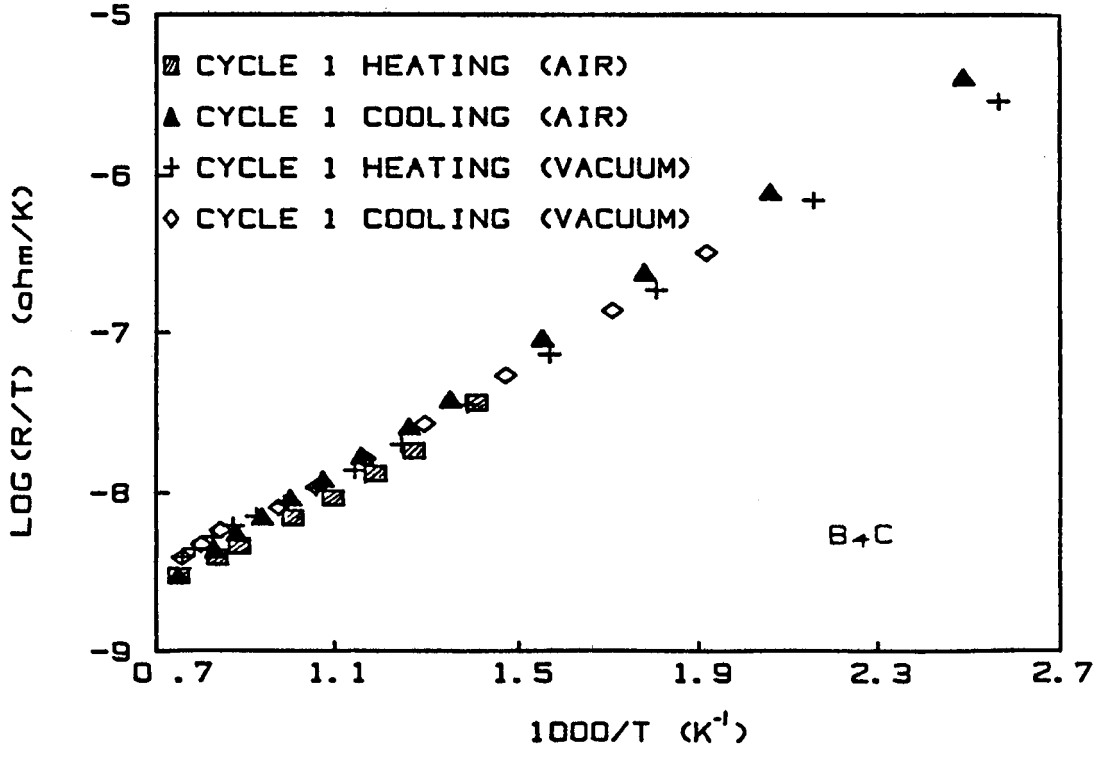

Fig. 20. Log(R/T) vs. 1/T for B_4C tested in air and in vacuum. Data are from the first cycle of heating and cooling.

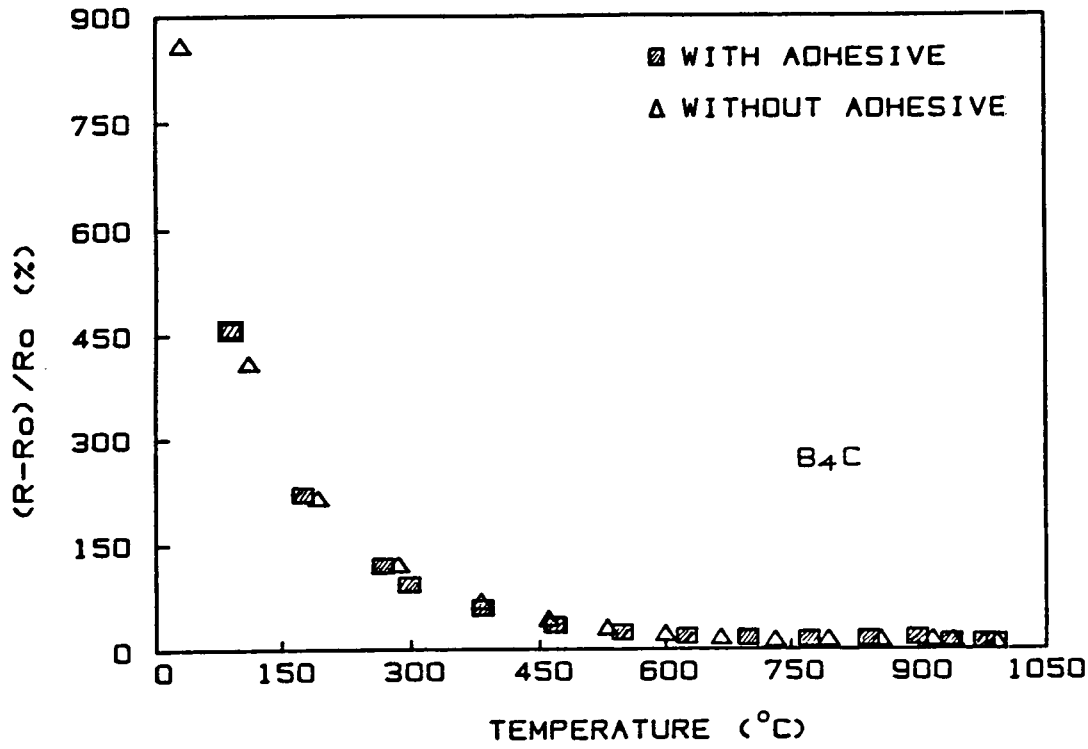

Fig. 21. Comparison the change in resistance with temperature of two B_4C: one with adhesive and one without

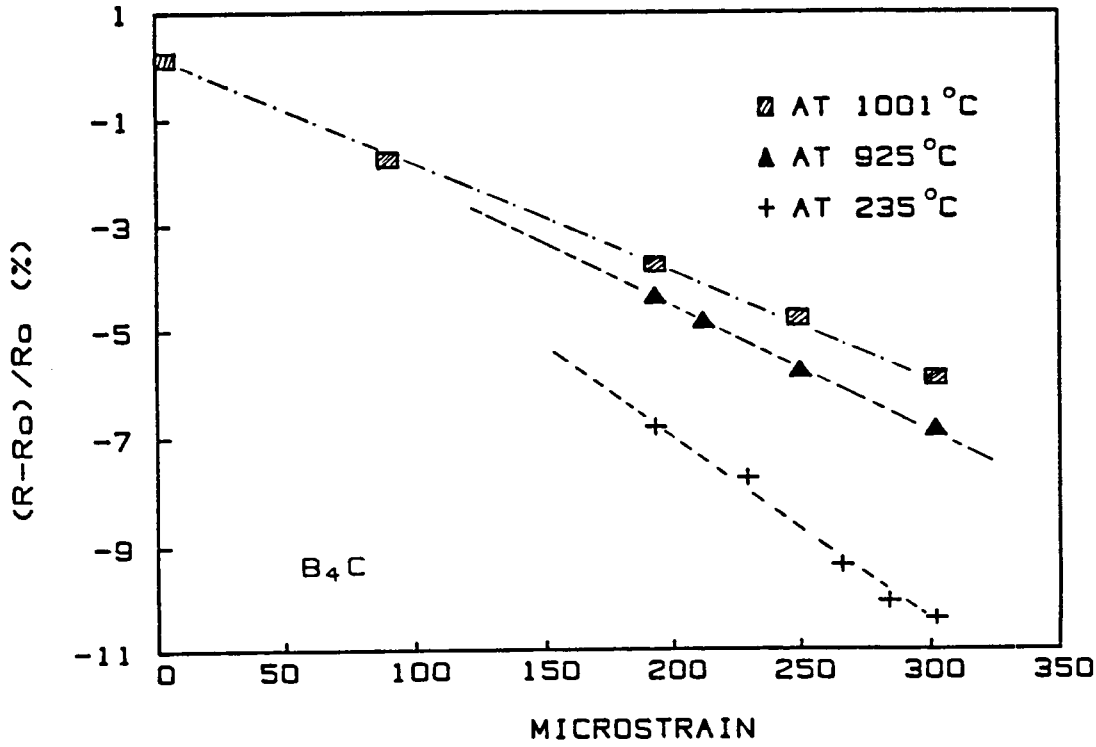

Fig. 22. Resistance vs. strain at three temperatures for B_4C. Resistance is normalized to its value under no strain.

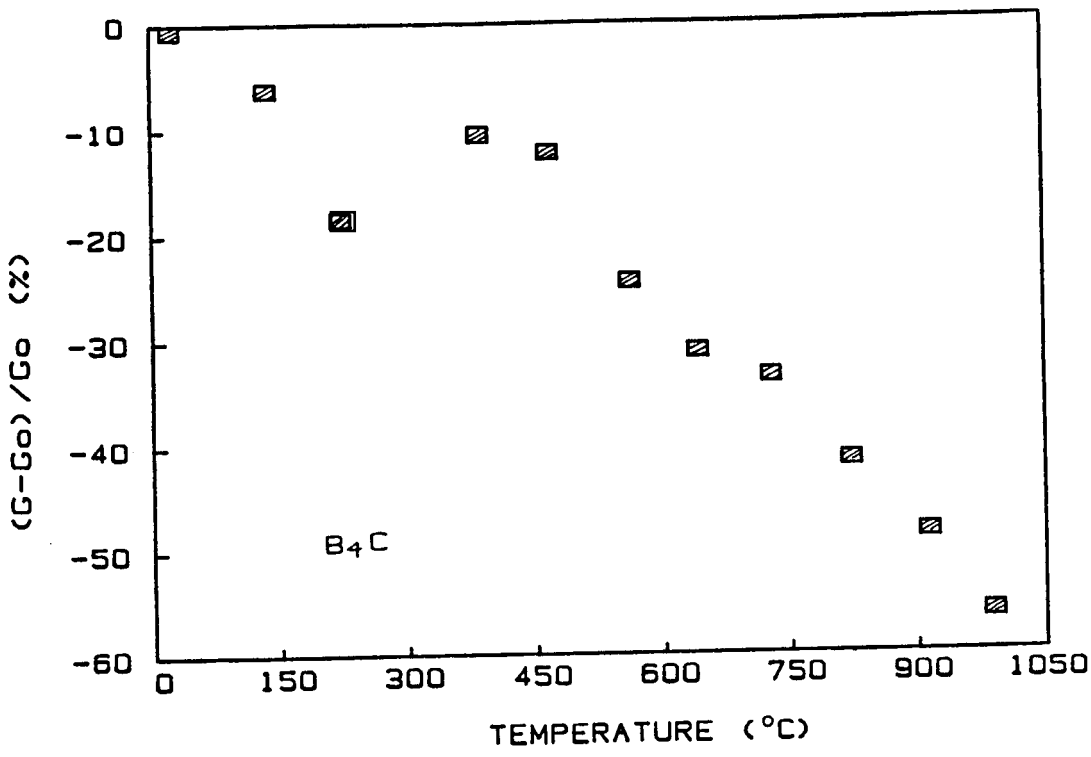

Fig. 23. Gage factor vs. temperature for boron carbide.